Inorg. Chem. **2005**, *44*, 5882–5889

High-Throughput Investigation and Characterization of Cobalt Carboxy Phosphonates

Sebastian Bauer,[†] Thomas Bein,[‡] and Norbert Stock*,[†]

Institute of Inorganic Chemistry, Christian-Albrechts-University, Otto-Hahn-Platz 6/7, D 24118 Kiel, Germany, and Department of Chemistry and Biochemistry, Ludwig-Maximilians-University, Butenandtstrasse 5-13 (E), D 81377 Munich, Germany

Received April 5, 2005

High-throughput methods have been employed to study the system $Co^{2+}/(H_2O_3PCH_2)_2NCH_2C_6H_4COOH/NaOH$ in detail. The use of the phosphonocarboxylic acid $(H_2O_3PCH_2)_2NCH_2C_6H_4COOH$ has led to several new cobalt carboxyaryl phosphonates under hydrothermal conditions. In addition to the effect of the pH of the starting mixture, the influence of the counterions of the cobalt salts on the product formation was investigated. Thus, reaction trends as well as fields of formation could be identified. Four new compounds $Co_2[(O_3PCH_2)_2NCH_2C_6H_4COOH]\cdot H_2O$ (**1**), $Co[(O_3PCH_2)(OCH)NCH_2C_6H_4COOH]\cdot H_2O$ (**2**), $Co[H_2(O_3PCH_2)_2NCH_2C_6H_4COOH]$ (**3**), and $[Co_2(O_3PCH_2)_2NCH_2C_6H_4COOH]\cdot 3.5H_2O$ (**4**) were obtained, and compounds **1** and **2** could be isolated as single crystals suitable for single-crystal X-ray diffraction. The counterions of the cobalt salts have an influence on the structure of the resulting compounds. This is due to the effect on the initial pH as well as the possibility of the counterions to take part in redox reactions. Compounds **1** and **4** are formed under more basic conditions, and the phosphonic acid group is fully deprotonated. The structure of **1** is a rare example of the family of inorganic–organic hybrid materials with iminobis(methylphosphonic acid) units wherein the nitrogen coordinates to the metal center. Compound **2** is the result of an in situ oxidation of one of the P–C bonds; the organic building unit is stabilized by complexation of the cobalt ion. On the basis of spectroscopic, thermogravimetric, elemental chemical analysis, and EDX-analysis data, compound **3** has been characterized as $Co[H_2(O_3PCH_2)_2NCH_2C_6H_4COOH]$ and compound **4** as $[Co_2(O_3PCH_2)_2NCH_2C_6H_4COOH]\cdot 3.5H_2O$. X-ray powder diffraction and IR-spectroscopic studies show that thermal treatment of **4** leads to the title compound **1**. This transformation is accompanied by a change of color from pink to deep blue.

Introduction

High-throughput methods applied to materials discovery have attracted much attention over the past few years[1,2] because they permit a fast and efficient investigation of parameter space while consuming only small amounts of starting materials. Whereas the first investigations regarding the discovery and optimization of solid-state materials were based on thin-film techniques or high-temperature oxide chemistry, the introduction of high-throughput methods incorporating hydrothermal syntheses has been especially challenging. With a varying degree of miniaturization and automation, the proof of concept was first given through the investigation of known microporous materials,[3,4,5,6] but recently also new zinc phosphates,[7,8] a new manganese arsenate,[9] and a number of metal phosphonates as well as

* Author to whom correspondence should be addressed. E-mail: stock@ac.uni-kiel.de. Tel.: +49-431-880-1675. Fax.: +49-431-880-1775.
[†] Christian-Albrechts-University.
[‡] Ludwig-Maximilians-University.

(1) Bein, T. *Angew. Chem., Int. Ed.* **1999**, *38*, 323.
(2) Cong, P. J.; Doolen, R. D.; Fan, Q.; Giaquinta, D. M.; Guan, S. H.; McFarland, E. W.; Poojary, D. M.; Self, K.; Turner, H. W.; Weinberg, W. H. *Angew. Chem., Int. Ed.* **1999**, *38*, 483.
(3) Akporiaye, D. E.; Dahl, I. M.; Karlsson, A.; Wendelbo, R. *Angew. Chem., Int. Ed. Engl.* **1988**, *37*, 3369.
(4) Klein, J.; Lehmann, C. W.; Schmidt, H. W.; Maier, W. F. *Angew. Chem., Int. Ed.* **1998**, *37*, 3369.
(5) Choi, K.; Gardner, D.; Hilbrandt, N.; Bein, T. *Angew. Chem., Int. Ed.* **1999**, *38*, 2891.
(6) Lai, R.; Kang, B. S.; Gavalas, G. R. *Angew. Chem., Int. Ed.* **2001**, *40*, 408.
(7) Song, Y.; Yu, J.; Li, G.; Li, Y.; Wang, Y.; Xu, R. *Chem. Commun.* **2002**, 1720.
(8) Song, Y.; Yu, J.; Li, G.; Li, Y.; Wang, Y.; Xu, R. *Eur. J. Inorg. Chem.* **2004**, 3718.
(9) Stock, N.; Bein, T. *Solid State Sci.* **2003**, *5*, 1207.

10.1021/ic0505089 CCC: $30.25
Published on Web 07/09/2005

metal phosphonocarboxylates[10,11] have been obtained. We have developed a multiclave that allows the investigation of 48 different hydrothermal reactions at a time.[9,10] The methodology includes automatic dispensing of solids and liquids, followed by homogenization, pH-measurement, synthesis, isolation, and washing, as well as automated phase analysis by X-ray diffraction, without the manipulation of individual samples.

There has been rising interest in the synthesis of new metal phosphonates in recent years. A certain control of the dimensionality of the formed structures by suitable choice of the phosphonic acid leads to the potential application of metal phosphonates in the areas of catalysis, ion exchange, intercalation chemistry, and charge storage.[12,13] Not only the phosphonic acid but many parameters such as metal ion, synthesis temperature, and pH value have an influence on the product formed. Nevertheless, systematic investigations of the synthesis fields were rarely presented due to the complexity of the systems. Thus, high-throughput methods are ideal.

While a large number of carboxylic, phosphonic, and phosphonocarboxylic acids have been employed in the synthesis of three-dimensional (3D) framework structures in the past few years,[14−16] we have focused our attention on the use of polyphosphonic and phosphonocarboxylic acids as organic building units. In particular, we are interested in polyfunctional phosphonic acids containing iminobis(methylphosphonic acid) units, $(H_2O_3PCH_2)_2N$. To understand the influence of the organic group, R, in $(H_2O_3PCH_2)_2N$-R we have recently started a systematic investigation in the application of fuctionalized iminobis(methylphosphonic acid) derivatives for the synthesis of metal phosphonates. Thus, by reacting $(H_2O_3PCH_2)_2N(CH_2)_4N(CH_2PO_3H)_2$,[10,17] and $(H_2O_3PCH_2)_2NCH_2C_6H_4CH_2N(CH_2PO_3H)_2$[18] with different metal ions, we obtained a number of new compounds, some containing three-dimensional framework structures and one showing reversible dehydration/hydration properties.[18] Other groups introduced a flexible carboxylic acid moiety, employing $(H_2O_3PCH_2)_2NCH_2COOH$[19] and $(H_2O_3PCH_2)_2NC_3H_6$-COOH.[20] This has resulted in a number of 3D network and layered structures. In the ligand $(H_2O_3PCH_2)_2NCH_2C_6H_4$-COOH ($H_5L$) the carboxylic acid group separated from the bis(phosphonic acid) group by means of the phenyl group. This rigid moiety in combination with the flexible coordination properties of the iminobis(methylphosphonic acid) and carboxylic acid functionality makes H_5L a promising candidate for the synthesis of new metal phosphonates with interesting structural features. Since limited information on the chemistry of the ligand H_5L is available,[21] we employed high-throughput methods to systematically study its coordination behavior using different metal ions. Herein we report the results of the investigation on the system Co^{2+}/H_5L/NaOH. The variation of the counterion of the cobalt source as well as the gradual change of the pH led to four new compounds $Co_2[(O_3PCH_2)_2NCH_2C_6H_4COOH]\cdot H_2O$ (**1**), $Co[(O_3PCH_2)(OCH)NCH_2C_6H_4COOH]\cdot H_2O$ (**2**), $Co[H_2(O_3PCH_2)_2NCH_2C_6H_4COOH]$ (**3**), and $[Co_2(O_3PCH_2)_2NCH_2C_6H_4COOH]\cdot 3.5H_2O$ (**4**). Additional information on the thermal behavior as well as the IR spectra is presented.

Experimental Section

Materials and Methods. All chemicals were obtained from commercial sources and used without further purification. High-throughput X-ray analysis was carried out using a newly developed STOE instrument based on a STADI P diffractometer for high-throughput measurements in transmission geometry and equipped with an image-plate detector system.[10] The data collection time was 6 min/sample. High-precision X-ray powder diffraction patterns were recorded with a STOE STADI P diffractometer using monochromated Cu $K\alpha_1$ radiation. IR spectra were recorded on a Bruker IFS 66v/S FTIR spectrometer in the spectral range 4000−400 cm^{-1} using the KBr disk method. Thermogravimetric analyses were carried out in air (25 cm^3/min, 30−600 °C, 10 °C/min) using a NETZSCH STA 449C analyzer. The SEM micrographs and the EDX analyses were obtained using a JEOL 6500F field-emission scanning electron microscope equipped with an Oxford EDX detector system. Solution NMR was recorded on a JEOL GSX 270, using D_2O/NaOH as solvent. H_3PO_4 (85%) was used as ^{31}P substitutive reference. Carbon, hydrogen, and nitrogen contents were determined by elemental chemical analysis on an Elementar Vario EL analyzer.

Synthesis of $(H_2O_3PCH_2)_2NCH_2C_6H_4COOH$, H_5L. H_5L was prepared by reacting 4-(aminomethyl)benzoic acid (6.05 g, 40.0 mmol), phosphoric acid (6.56 g, 80.0 mmol), deionized water (20 cm^3), concentrated hydrochloric acid (10 cm^3), and paraformaldehyde (8.1 cm^3 of a 38 wt % aqueous solution, 100 mmol), according to a procedure described in the literature.[22] The reaction product was recrystallized from 600 cm^3 of deionized water. The assignations for ^1H, ^{13}C, and ^{31}P in D_2O/NaOH are as follows (Figure 1). ^1H NMR: $\delta = 2.45$ (d, 4 H, $^2J(P-H) = 11.5$ Hz, $-CH_2PO(OH)_2$), 3.78 (s, 2 H, $-CH_2N-$), 7.37 (d, 2H, $^3J_{H,H} = 7.2$ Hz, C4−H and C4′−H), 7.65 (d, 2H, $^3J_{H,H} = 6.8$ Hz, C3−H and C3′−H) ppm. ^{13}C NMR: $\delta = 54.9$ (dd, $^1J_{C,P}$ (C7/7′−P) = 145 Hz, $^3J_{C,P}$ (C7/7′−P) = 8.2 Hz), 60.1 (m, C6), 129.0 ppm (s, C4/4′), 130.0 (s, C3/3′), 134.8 (s, C5), 142.2 (s, C2), 175.7 (s, C1) ppm. ^{31}P NMR: 17.49 ppm (s).

(10) Stock, N.; Bein, T. *Angew. Chem.* **2004**, *116*, 767; *Angew. Chem., Int. Ed.* **2004**, *43*, 749.
(11) Stock, N.; Bein, T. *J. Mater. Chem.* **2005**, *15*, 1384.
(12) Cheetham, A. K.; Férey, G.; Loiseau, T. *Angew. Chem., Int. Ed.* **1999**, *38*, 3268.
(13) Clearfield, A. Metal Phosphonate Chemistry. In *Progress in Inorganic Chemistry*; K. D., Ed.; John Wiley: New York, 1998; Vol. 47, pp 371−510.
(14) (a) Stock, N.; Frey, S.; Stucky, G. D.; Cheetham, A. K. *J. Chem. Soc., Dalton Trans.* **2000**, 4292. (b) Stock, N.; Stucky, G. D.; Cheetham, A. K. *Chem. Commun.* **2000**, 2277. (c) Stock, N. *Solid State Sci.* **2002**, *4*, 1089. (d) Stock, N.; Bein, T. *J. Solid State Chem.* **2002**, *167*, 330.
(15) (a) Rosi, N. L.; Eddaoudi, M.; Kim, J.; O'Keeffe, M.; Yaghi, O. M. *Angew. Chem.* **2002**, *114*, 294; *Angew. Chem., Int. Ed.* **2002**, *41*, 284. (b) Eddaoudi, M.; Moler, D. B.; Li, H.; Chen, B.; Reineke, T. M.; O'Keeffe, M.; Yaghi, O. M. *Acc. Chem. Res.* **2001**, *34*, 319.
(16) Millange, F.; Serre, C.; Ferey, G. *Chem. Commun.* **2002**, 822. Barthelet, K.; Marrot, J.; Riou, D.; Ferey, G. *Angew. Chem.* **2002**, *114*, 291; *Angew. Chem., Int. Ed.* **2002**, *41*, 281.
(17) Stock, N.; Rauscher, M.; Bein, T. *J. Solid State Chem.* **2004**, *177*, 642.
(18) Stock, N.; Stoll, A.; Bein, T. *Microporous Mesoporous Mater.* **2004**, *69*, 65.
(19) Mao, J.-G.; Wang, Z.; Clearfield, A. *New J. Chem.* **2002**, *26*, 1010.
(20) Constantino, U.; Nocchetti, M.; Vivani, R. *J. Am. Chem. Soc.* **2002**, *124*, 8428.
(21) Song, J.-L.; Prosvirin, A. V.; Zhao, H.-H.; Mao, J.-G. *Eur. J. Chem.* **2004**, 3706.
(22) Moedritzer, K.; Irani, R. R. *J. Org. Chem.* **1966**, *31*, 1603.

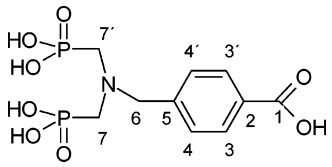

Figure 1. Scheme for 4-{[bis(phosphonomethyl)amino]methyl}benzoic acid.

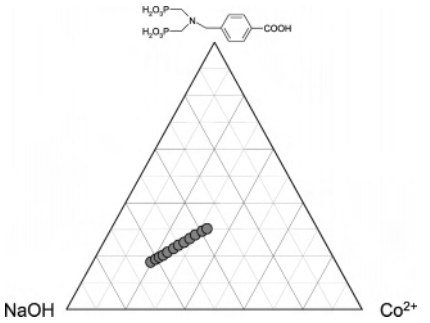

Figure 2. Ternary diagram with 12 different ratios of $NaOH/H_5L/Co^{2+}$. Four Co^{2+} sources, $CoCl_2$, $Co(O_2CCH_3)_2$, $Co(NO_3)_2$, and $CoSO_4$, were used resulting in 48 individual reactions.

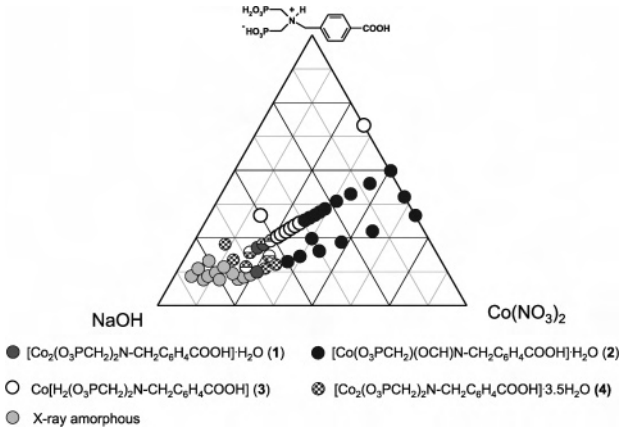

Figure 3. Crystallization diagram for the system $Co(NO_3)_2/H_5L/NaOH$. Results are based on a powder-XRD investigation.

High-Throughput Experiments. The system $Co^{2+}/H_5L/NaOH$ was investigated using high-throughput methods. The first high-throughput experiment was set up to study the influence of the anion of the cobalt salt on the reaction products. Thus, four different Co^{2+} compounds ($CoCl_2$, $Co(O_2CCH_3)_2$, $Co(NO_3)_2$, and $CoSO_4$) were reacted (T = 170 °C, 72 h) at a constant metal:H_5L = 1:1 ratio and the amount of NaOH was subsequently varied in 12 steps (Figure 2). The water content for all experiments was set to 98.8 mol %.

To gain a better understanding of the products formed within the system $Co(NO_3)_2/H_5L/NaOH$, a second high-throughput experiment was designed. Thus, 48 different $Co(NO_3)_2/H_5L/NaOH$ ratios at a constant water content of 99.2 mol % were set up and reacted under hydrothermal conditions (T = 160 °C, 72 h). The corresponding crystallization diagram is shown in Figure 3. Exact amounts of the starting materials in the individual mixtures are given in the Supporting Information.

X-ray Structure Analysis. Suitable single crystals were carefully selected using a polarizing microscope. Single-crystal structure determinations by X-ray diffraction were performed on a STOE IPDS diffractometer equipped with a fine-focus sealed tube X-ray source (Mo Kα radiation, λ = 71.073 pm) operating at 55 kV and 50 mA. For data reduction and the absorption correction the program Xred was used.[23] The single-crystal structures were solved by direct methods and refined using the program package SHELX-TL.[24] For **1** and **2**, all H atoms bound to carbon atoms were placed onto calculated positions. These H atoms were refined using a riding model and fixing the temperature factor to be 1.2 times the value of the atom they are bonded to. Additionally, for **2,** hydrogen atoms of the carboxylic acid group and the H_2O molecule were located from the difference Fourier maps. The hydrogen bonds were calculated using Platon.[25] Crystallographic data are given in Table 1. Selected bond distances and angles are listed in Tables 2and 3.

Table 1. Summary of Crystal Data, Intensity Measurement, and Structure Refinement Parameters for $Co_2[(O_3PCH_2)_2NCH_2C_6H_4COOH]\cdot H_2O$ (**1**) and $Co[(O_3PCH_2)(OCH)NCH_2C_6H_4COOH]\cdot H_2O$ (**2**)

param	**1**	**2**
cryst system	monoclinic	triclinic
space group	$P2_1/a$	$P\bar{1}$
a (pm)	1009.3 (1)	539.03(4)
b (pm)	952.24(6)	546.87(4)
c (pm)	1554.1 (2)	2111.6(2)
α (deg)		92.56(1)
β (deg)	99.97(1)	96.13 (1)
γ (deg)		107.771(9)
V (10^6 pm^3)	1471.1(2)	587.39(8)
Z	4	2
formula mass (g/mol)	471.01	348.11
ρ (g/cm^3)	2.127	1.968
F(000)	944	354
cryst size (mm^3)	0.22 × 0.09 × 0.03	0.20 × 0.08 × 0.03
μ (mm^{-1})	2.522	1.631
abs corr	numerical	numerical
$T_{min.}/T_{max}$	0.7415/0.9290	0.9026/0.9820
θ range (deg)	2.52−27.93	2.92−27.99
range in hkl	$-13 \le h \le 13$, $-11 \le k \le 12$, $-20 \le l \le 20$	$-7 \le h \le 7$, $-7 \le k \le 6$, $-27 \le l \le 27$
tot. data collcd	12 293	5444
unique/obsd data ($I > 2\sigma(I)$)	3507/2023	2615/2068
extinctn coeff	0.0075(9)	none
R(int)	0.1471	0.0474
R1, wR2 ($I > 2\sigma(I)$)	0.0553, 0.1182	0.0338, 0.0817
R1, wR2 (all data)	0.1068, 0.1309	0.0464, 0.0855
goodness of fit	0.896	0.953
no. of variables	218	190
Δe min/max (10^6 e pm^{-3})	−1.193/1.216	−1.020/0.812

Table 2. Selected Bond Distances and Bond Angles $Co_2[(O_3PCH_2)_2NCH_2C_6H_4COOH]\cdot H_2O$ (**1**)

Bond Distances (pm)			
Co1−O (5×)	191.6(5)−235.6(4)	Co2−O (5×)	202.6(4)−222.9(4)
		Co2−N1	221.1(5)
P1−O1	153.5(4)	P2−O4	153.4(4)
P1−O2	151.5(4)	P2−O5	149.8(5)
P1−O3	151.2(4)	P2−O6	152.9(4)
P1−C1	181.5(7)	P2−C2	181.1(6)
N1−C1	150.0(7)	N1−C3	147.2(8)
N1−C2	148.2(8)	C3−C4	1501(9)
$C-C_{phenyl}$ (6×)	138(1)−140(1)	C7−C10	154(1)
C10−O7	121(1)	C10−O8	131(1)

Bond Angles (deg)			
O−P−C	102.0(2)−111.9(3)	O−P−O	109.1(2)−114.6(2)
O7−C10−O8	125.5(9)	C−N−C	108.5(4)−117.6(5)
O8−C10−C7	113.6(7)		

(23) *XRED, data reduction and absorption correction program*, version 1.09 for Windows; Stoe & Cie GmbH: Darmstadt, Germany, 1997.
(24) Sheldrick, G. M. *SHELXTL-PLUS Crystallographic System*; Siemens Analytical X-ray Instruments, Inc.: Madison, WI, 1992.
(25) SPEK, A. L. *Platon-92*; University of Utrecht: Utrecht, The Netherlands, 1992.

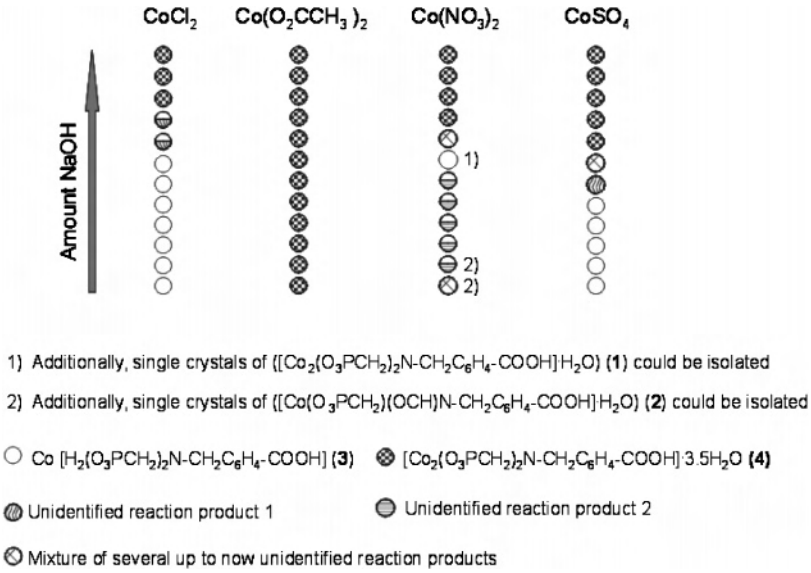

Figure 4. Crystallization diagram of the system $Co^{2+}/H_5L/NaOH$ using four different cobalt sources. Results are based on a powder-XRD investigation. The molar ratios for each system are shown in Figure 2.

Table 3. Selected Bond Distances and Bond Angles for $Co[(O_3PCH_2)(OCH)NCH_2C_6H_4COOH]\cdot H_2O$ (**2**)

Bond Distances (pm)			
Co−O (6×)	205.4(2)−224.6(2)	P1−O2	151.5(2)
P1−O1	151.7(2)	P1 − O3	153.4(2)
P1−C1	182.6(3)	N1 − C1	145.8(3)
N1−C2	129.5(3)	N1 − C3	146.5(3)
C2−O4	125.9(3)	C3 − C4	151.1(4)
$C-C_{phenyl}$ (6×)	138.2(5)−139.9(5)	C7 − C10	148.6(4)
C10−O5	125.5(5)	C10 − O6	127.2(4)

Bond Angles (deg)			
O−P−C	104.2(1)−107.5(1)	O−P−O (3×)	110.8(1)−114.0(1)
O4−C2−N1	115.6(2)	C−N−C	116.6(2)−123.6(2)
O6−C10−C7	116.5(3)	O5−C10−O6	124.3(3)
O5−C10−C7	119.2(3)		

Results and Discussion

High-Throughput Investigation. The synthesis field was investigated using two high-throughput experiments. In the study four new compounds were unequivocally identified. While **1** and **2** were obtained as single-crystalline products, compounds **3** and **4** were isolated as microcrystalline products, which were characterized in detail using elemental and thermogravimetric analysis as well as IR spectroscopy. The results of the first high-throughput experiment are shown in Figure 4. For the systems $Co^{2+}/H_5L/NaOH$ with $CoCl_2$ and $CoSO_4$ as starting salts a clear dependency on the intial pH of the product formed is observed. At low pH each phosphonate group is monodeprotonated and $Co[H_2(O_3PCH_2)_2NCH_2C_6H_4COOH]$ (**3**) is formed as derived from EDX data (ratio Co/P = 1/2), elemental chemical analysis (Anal. Found: C, 30.20; H, 3.55; N, 3,47. Calcd: C, 30.32; H, 3.31; N, 3.54), and TG and IR data (see thermal and IR spectroscopy study section). With increasing pH further deprotonation of the phosphonic acid takes place and $[Co_2(O_3PCH_2)_2NCH_2C_6H_4COOH]\cdot 3.5H_2O$ (**4**) is obtained. The composition of **4** is supported by EDX data (ratio Co/P = 1/1), elemental chemical analysis (Anal. Found: C, 24.48; H, 3.28; N, 2.71. Calcd: C, 23.27; H, 3.52; N, 2.79), and

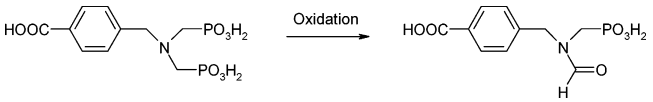

Figure 5. Scheme for the oxidation of H_5L resulting in formamide-derivative H_3L^{ox} acting as a new ligand with Co^{2+} as observed in $Co[(O_3PCH_2)(OCH)NCH_2C_6H_4COOH]\cdot H_2O$ (**2**).

TG and IR data. In the case of cobalt acetate as the starting material, the initial pH is higher from the beginning due to the hydrolysis reaction of the acetate ion. Therefore, within the investigated parameter space only $[Co_2(O_3PCH_2)_2NCH_2C_6H_4COOH]\cdot 3.5H_2O$ (**4**) is observed. With employment of $Co(NO_3)_2$ as the Co^{2+} source, the system is more complex and new additional phases are observed. At higher initial pH $[Co_2(O_3PCH_2)_2NCH_2C_6H_4COOH]\cdot 3.5H_2O$ (**4**) is formed as expected, but at lower pH values the formation of additional compounds takes place. Thus, single crystals of the side products, $Co_2[(O_3PCH_2)_2NCH_2C_6H_4COOH]\cdot H_2O$ (**1**) and $Co[(O_3PCH_2)(OCH)NCH_2C_6H_4COOH]\cdot H_2O$ (**2**), could be isolated. The composition of **1** suggests it to be the dehydration compound of **4**. The single-crystal analysis of **2** revealed an interesting formation process. Thus, an in situ oxidation of the ligand H_5L led to the formation of a new ligand $(H_2O_3PCH_2)(OCH)NCH_2C_6H_4COOH$ (H_3L^{ox}), a formamide derivative (Figure 5), which is stabilized under the reaction conditions by complexation and the formation of the title compound **2**.

The second high-throughput experiment was set up to further elucidate the system $Co(NO_3)_2/H_5L/NaOH$. Using exclusively $Co(NO_3)_2$ as a starting material, the pH-dependent product formation was confirmed. Thus, $[Co_2(O_3PCH_2)_2NCH_2C_6H_4COOH]\cdot 3.5H_2O$ (**4**) is formed at higher initial pH values whereas $Co[H_2(O_3PCH_2)_2NCH_2C_6H_4COOH]$ (**3**) occurs at initial compositions with a lower amount of NaOH. In addition, the synthesis conditions for $Co_2[(O_3PCH_2)_2NCH_2C_6H_4COOH]\cdot H_2O$ (**1**) and $Co[(O_3PCH_2)(OCH)NCH_2C_6H_4COOH]\cdot H_2O$ (**2**) were optimized and their fields of formation identified. Some products that were found in the

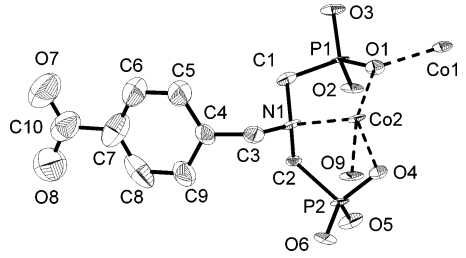

Figure 6. Asymmetric unit of $Co_2[(O_3PCH_2)_2NCH_2C_6H_4COOH]\cdot H_2O$. Thermal ellipsoids are shown at the 85% probability level.

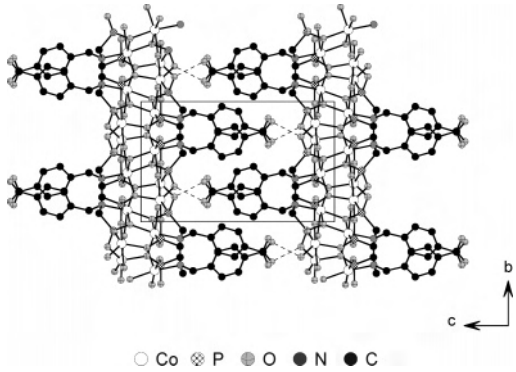

Figure 7. View of the structure of $Co_2[(O_3PCH_2)_2NCH_2C_6H_4COOH]\cdot H_2O$ (**1**) in the *b*,*c*-plane.

first experiment did not form within the observed parameters in the second high-throughput experiment. This could be due to the lower reaction temperatures employed in the second high-throughput investigation.

Crystal Structure of $Co_2[(O_3PCH_2)_2NCH_2C_6H_4COOH]\cdot H_2O$ (1). The asymmetric unit of $Co_2[(O_3PCH_2)_2NCH_2C_6H_4COOH]\cdot H_2O$ contains 24 crystallographically independent non-hydrogen atoms (Figure 6). The crystal structure is comprised of two crystallographic independent Co^{2+}, one $[(O_3PCH_2)_2NCH_2C_6H_4COOH]^{4-}$ ion, and one water molecule. Co(1) ions are surrounded by five oxygen atoms, whereas the Co(2) centers are coordinated by five oxygen atoms and one nitrogen atom forming distorted octahedra (Supporting Information, Figure S1). The Co−O distances are in the range 1.91.6(5)−235.6(4) pm and correspond well with those reported in other cobalt phosphonates.[21] The Co−N distance (221.1(5) pm) is in the same range and represents a rare example of iminobis(methylphosphonic acid) compounds where the nitrogen is involved in coordination of the metal centers.[26,21] Two edge-sharing $Co(2)O_5N$ octahedra are further connected by two Co(1) polyhedra corner-sharing oxygen atoms forming $Co_4O_{14}N_2$ units (Figure S2). Tetrameric $Co_4O_{14}N_2$ units are connected by phosphonate groups, and layers in the *a*,*b*-plane are formed (Figure 7). The phenylcarboxylic acid groups are oriented perpendicular to the layers. Thus, these layers are connected through hydrogen bonds between the carboxylic acid group and the phosphonate group $P(2)O_3^{2-}$ (Figure 7). This is supported by the O(8)−O(6) distance (270.9 pm) (Figure S3). The C−O distances of C(10)−O(8) = 131(1) pm and C(10)−O7 = 121(1) pm correspond to C−O single and C−O double bonds, respectively.

(26) Makaranets, B. I.; Polynova, T. N.; Mitrofanova, N. D.; Porai-Koshits, M. A. *J. Struct. Chem.* **1991**, 94.

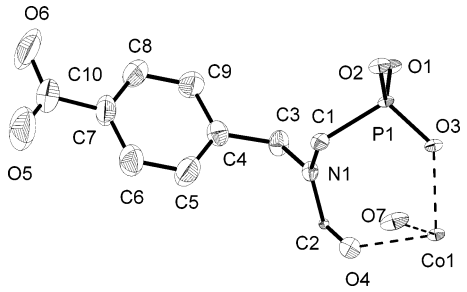

Figure 8. Asymmetric unit of $Co[(O_3PCH_2)(OCH)NCH_2C_6H_4COOH]\cdot H_2O$ (**2**). Thermal ellipsoids are shown at the 85% probability level.

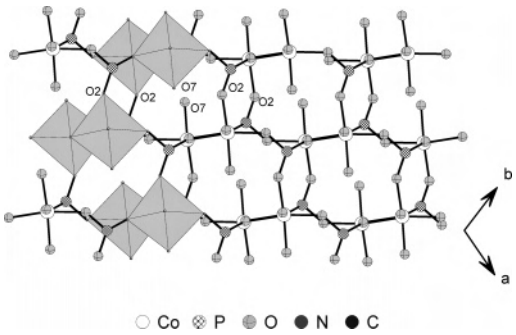

Figure 9. Co_2O_{10} units forming a strand along the *b*-axis (gray pairs of octahedra) and connection of the strands via O(2) to form a 2D-network parallel to the *a*,*b*-plane in $Co[(O_3PCH_2)(OCH)NCH_2C_6H_4COOH]\cdot H_2O$ (**2**).

Table 4. Hydrogen Bonds (Bond Distances in pm, Angles in deg) for $Co[(O_3PCH_2)(OCH)NCH_2C_6H_4COOH]\cdot H_2O$ (**2**) (D = Proton Donor, A = Proton Acceptor)

D−H···A	D−H	H···A	D···A	<D−H···A
O6−H6···O5[a]	84(2)	180(2)	263.4(4)	263.4(4)
O7−H71···O2	84(4)	192(4)	271.9(3)	271.9(3)
O7−H71···O3[b]	84(4)	253(4)	301.4(3)	301.4(3)
O7−H72···O1[b]	90(4)	190(4)	272.5(3)	272.5(3)

[a] $1-x, 3-y, -z$. [b] $x, 1+y, z$.

Crystal Structure of $Co[(O_3PCH_2)(OCH)NCH_2C_6H_4COOH]\cdot H_2O$ (2). The asymmetric unit of $Co[(O_3PCH_2)(OCH)NCH_2C_6H_4COOH]\cdot H_2O$ is shown in Figure 8. The structure is built up from one crystallographically independent Co^{2+} cation, one $[(O_3PCH_2)(OCH)NCH_2C_6H_4COOH]^{2-}$ anion, and one water molecule that is coordinatively bound to the Co^{2+} ion. The cobalt atoms are surrounded by six oxygen atoms and form edge-sharing octahedral dimers, Co_2O_{10} units (Figure S4). All oxygen atoms of the phosphonate group, the oxygen of the formamide group, and oxygen atom O(7) of the water molecule take part in the coordination of the Co^{2+} ion. The Co_2O_{10} units are connected via the phosphonate groups and cobalt phosphonate layers parallel the *a*,*b*-plane are formed (Figure 9). Hydrogen bonds (Table 4) between the oxygen O(7) of the water molecule and the phosphonate oxygens O(1) and O(2) further stabilize the network (Figure S5). The layers are interconnected via hydrogen bonds between the carboxylic acid groups that are oriented perpendicular to the layers and point to those of the successive layer (Figure 10).

Thermal Study. The thermal properties of the title compounds were studied by employing thermogravimetric

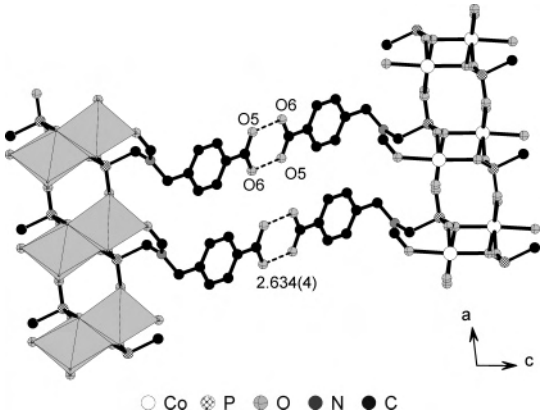

Figure 10. Interconnection of two parallel layers by hydrogen bonding via carboxylic acid groups in $Co[(O_3PCH_2)(OCH)NCH_2C_6H_4COOH]\cdot H_2O$ (**2**).

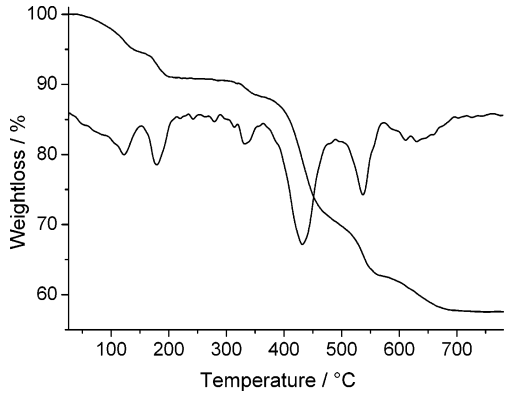

Figure 11. TG diagram with derivative of $[Co_2(O_3PCH_2)_2NCH_2C_6H_4COOH]\cdot 3.5H_2O$ (**4**).

measurements. Compound **1** shows no significant weight loss up to 310 °C. Between 310 and 370 °C a weight loss of 3.4% occurs. This can be assigned to the loss of one lattice water molecule (expected 3.8%). Upon further heating three more steps of weight losses are observed. This is due to the condensation of the carboxylic acid groups, decomposition, and pyrolysis, respectively. For **2,** no thermogravimetric measurements were carried out because examination under the microscope revealed that it is accompanied by small amounts of amorphous byproducts, which would complicate the experiment. The fact that the TG of **3** (Figure S6) shows no significant weight loss up to 150 °C together with the results of IR spectroscopic studies and results of elemental chemical analysis reveals that no lattice water molecules are present. Up to 330 °C a weight loss of 4.5% is observed, which correlates with the release of one water molecule/formula unit. However, no plateau with constant weight but a steady decrease in weight is observed. The thermal behavior of compound **4** is of special interest since the phase change is accompanied with color change from pink to deep blue (Figure S9). Therefore, additional experiments in a drying oven at 100, 110, 120, 150, and 190 °C were performed. The color change starts at about 110 °C and is complete at 190 °C. The TG diagram (Figure 11) of compound **4** shows six stages of weight loss. The first stage begins at 45 °C and is complete at 150 °C and corresponds to the loss of 1.5 lattice water molecules. The weight loss of 5.3% is in good

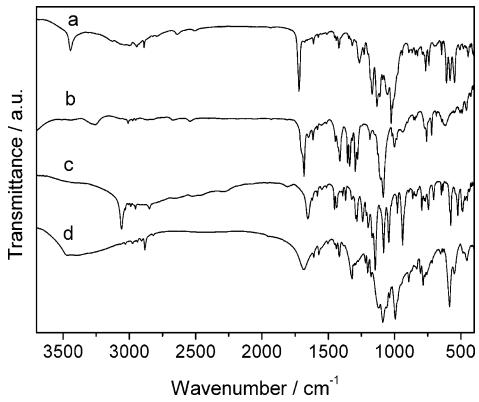

Figure 12. IR spectra for (a) $Co_2[(O_3PCH_2)_2NCH_2C_6H_4COOH]\cdot H_2O$ (**1**), (b) $Co[(O_3PCH_2)(OCH)NCH_2C_6H_4COOH]\cdot H_2O$ (**2**), (c) $Co[H_2(O_3PCH_2)_2NCH_2C_6H_4COOH]$ (**3**), and (d) $Co_2[(O_3PCH_2)_2NCH_2C_6H_4COOH]\cdot 3.5H_2O$ (**4**).

agreement with the calculated value (5.2%). The second step is observed between 150 and 210 °C and is due to the loss of one lattice water molecule. The experimental weight loss (3.8%) compares well with the expected weight loss (3.5%). Between 210 and 390 °C a weight loss of 3.8% (expected 3.5%) due to the release of the last lattice water molecule is observed. Upon further heating, condensation of the carboxylic acid groups and the decomposition and pyrolysis of the organic group take place, which can be recognized by three more steps of weight loss, which is completed at 750 °C with a total weight loss of 42.5%. The TG diagram of **4** beyond 200 °C compares well with the TG curve observed for **1**. Comparing XRD-powder patterns (Figure S7) and IR spectra of compound **4** heated to 190 °C with the corresponding data of compound **1** unambiguously shows the transformation of **4** to **1** by releasing 2.5 lattice water molecules. This structural transformation is accompanied by the coordination of nitrogen to the cobalt center, which leads to the change of the color from pink to blue.

IR Spectroscopic Study. All four title compounds were studied by IR spectroscopy. The spectra are shown in Figure 12. In accordance with the crystallographic results that the water molecules in $Co_2[(O_3PCH_2)_2NCH_2C_6H_4COOH]\cdot H_2O$ (**1**) are not involved in hydrogen bonding, a well-defined, narrow band at 3444 cm^{-1} is present. The corresponding deformation band appears at 1612 cm^{-1}. Bands in the region from 3045 to 2889 cm^{-1} are due to aromatic and aliphatic C−H stretching vibrations. The CH_2-deformation vibration appears at 1421 cm^{-1}. Several broad bands from 2800 to 2500 cm^{-1} may be assigned to O−H stretching vibrations of the carboxylic acid groups involved in hydrogen bonding. The C═O stretching vibration of the carboxylic acid group appears as a sharp band at 1721 cm^{-1}. This value indicates that the oxygen of the C═O group is not involved in hydrogen bonding, which is consistent with the X-ray investigations. Bands at 1266 and 1230 cm^{-1} can be assigned to P−C stretching vibrations. The set of bands between 1169 and 976 cm^{-1} is due to stretching vibrations of the tetrahedral CPO_3 groups.

To obtain a pure **2** for IR measurements crystals were separated from the amorphous byproduct under the micro-

scope. The broad adsorption bands at 3420 and 3271 cm^{-1} in the IR spectrum clearly show the presence of water molecules. The width suggest that the water is interacting through hydrogen bonds. The spectrum also shows the corresponding deformation band at 1615 cm^{-1}. The aromatic and aliphatic C−H stretching vibrations can be assigned to the bands at 3005, 2973, and 2951 cm^{-1}; the typical CH_2-deformation vibration can be found at 1412 cm^{-1}. The broad bands of low intensity at 2672 and 2544 cm^{-1} are most likely due to the O−H stretching vibrations of the carboxylic acid groups involved in hydrogen bonding. The C═O stretching vibration of the carboxylic acid group can be assigned to the sharp band at 1682 cm^{-1}. In comparison to compound **1** the band is shifted to lower wavenumbers due to the strong hydrogen bonds between two carboxylic acid groups that form dimeric units, whereas in **1** the carbonyl oxygen is not involved in hydrogen bonding. The shoulder at higher wavenumbers in the IR spectrum of **2** is most likely due to the C═O stretching vibration of the formamide group. The higher energy is consistent with the shorter bond distance found from crystallographic data. The band at 1448 cm^{-1} could be assigned to the C−C skeletal ring vibration mode. The bands at 1355 and 1339 cm^{-1} might be due to the C−O stretching vibrations of the carboxylic acid dimers.[27] Typical bands at 1298 and 1279 cm^{-1} can be assigned to P−C stretching vibrations. The sharp bands of high intensity between 1128 and 1085 cm^{-1} are due to PO_3 stretching vibrations.

The absence of bands correlated with vibration of water molecules in the IR spectrum of **3** indicates that no water is present in the structure. Several broad bands of low intensity in the region between 2700 and 2200 cm^{-1} (Figure S8) can be assigned to OH-stretching vibrations of P−OH and COOH groups with protons involved in hydrogen bonding.[28] The fairly broad band at 1655 cm^{-1} is assigned to the C═O stretching vibration of the carboxylic acid group. Its rather low position is typical for constellations where both oxygens of the COOH group participate in strong hydrogen bonds. The vibrations of the phosponic acid groups appear as a set of sharp bands in the region between 1200 and 1000 cm^{-1}.

The IR spectrum of **4** shows a broad and superimposed set of bands in the region above 3100 cm^{-1} indicating the presence of water molecules involved in hydrogen bonding. The absence of broad bands of low intensity in the range from 2700 to 2200 cm^{-1} indicates that no POH groups are present that form hydrogen bonding. The noticeable broad band of medium intensity of the C═O vibration of the carboxylic acid group is located at 1686 cm^{-1}; its form suggests that the COOH group is taking part in the formation of hydrogen bonds. The set of bands correlated to vibrations of the CPO_3 groups are observed in the region from 1200 to 1000 cm^{-1}.

The detailed thermal study of compound **4** was completed by IR measurements. In Figure 13 the IR spectra of **1** and **4** and that of **4** heated to 190 °C are plotted showing that the broad bands in **4** related to the water molecules and the carboxylic acid group upon heating transform into well-defined bands located at exactly the same positions such as those observed in the spectrum of **1**. Furthermore the spectra **1** and **4** treated at 190 °C are identical.

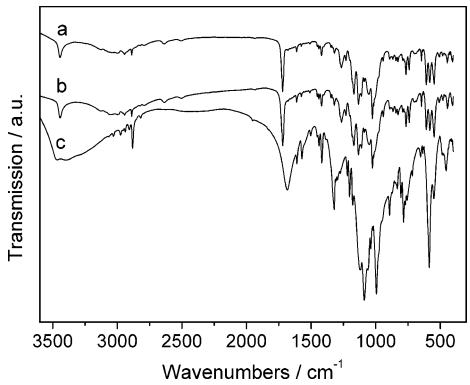

Figure 13. IR spectra for (a) $Co_2[(O_3PCH_2)_2NCH_2C_6H_4COOH]\cdot H_2O$ (**1**), (b) $Co_2[(O_3PCH_2)_2NCH_2C_6H_4COOH]\cdot 3.5H_2O$ (**4**) treated at 190 °C, and (c) $Co_2[(O_3PCH_2)_2NCH_2C_6H_4COOH]\cdot 3.5H_2O$ (**4**).

General Discussion. The application of our high-throughput methodology allows the systematic and rapid investigation of reactions under hydrothermal conditions. Low reagent consumption and the possibility to work under identical reaction conditions allow us to scan a larger part of the parameter space than would normally be possible. Thus, we are able to systematically investigate the influence of the cobalt counterion in the system $Co^{2+}/(H_2O_3PCH_2)_2NCH_2C_6H_4COOH$ (H_5L)/NaOH. We found similar trends in the product formation when starting from $CoCl_2$ and $CoSO_4$. Both, being salts of strong acids, generate similar initial pH values for equal molar ratios of reagents. The use of $Co(O_2CCH_3)_2$ as source of Co^{2+} leads to a higher initial pH value due to the hydrolysis reaction of the acetate ion. Thus, **4** is the only product formed within the investigated parameter space. In contrast, for synthesis starting with $CoCl_2$, $Co(NO_3)_2$, and $CoSO_4$ compound **4** appears only at higher molar ratios of NaOH. Surprisingly, the use of $Co(NO_3)_2$ under more acidic conditions led to two additional compounds $Co_2[(O_3PCH_2)_2NCH_2C_6H_4COOH]\cdot H_2O$ (**1**) and $Co[(O_3PCH_2)(OCH)NCH_2C_6H_4COOH]\cdot H_2O$ (**2**). Their crystal structures revealed two interesting features, i.e., in **1** the N atom is coordinated to the Co^{2+} ion. This leads to the deep blue color of the compound. Compound **2** is formed by the in situ oxidation of the P−C bond of the ligand H_5L, and the ligand H_3L^{ox} contains a formamide group. On the basis of detailed powder XRD, TG, and IR investigations and the observation of change of color during the thermal treatment of **4**, this compound was found to be the precursor compound for **1**. Thermal treatment at 190 °C results in a release of lattice water molecules, and the structure is transformed. The systematic investigation of the system $Co(NO_3)_2/(H_2O_3PCH_2)_2NCH_2C_6H_4COOH$ (H_5L)/NaOH by high-throughput methods allowed us to establish the fields of formation of the new cobalt phosphonocarboxylates. As expected, with increasing molar ratios of NaOH the grade

(27) Socrates, G. *Infrared and Raman Characteristic Group Frequencies*, 3rd ed.; Wiley: New York, 2002.
(28) Bellamy, L. J. *Infrared Spectra of Complex Molecules*; John Wiley and Sons: New York, 1958; Chapter 18.

of deprotonation of the ligand H_5L increases. Thus, the cobalt/H_5L ratio increases from one in compound **3** to two in compounds **1** and **4**. The unexpected oxidation of the phosphonocarboxylic acid takes place at rather low pH values according to the higher oxidation potential of the nitrate species under acidic conditions. Since $(H_2O_3PCH_2)_2NCH_2C_6H_4$-COOH proved to be a versatile ligand adopting different coordination modes that lead to interesting new structures, we are currently studying its use in the hydrothermal synthesis of other metal phosphonocarbxylates under hydrothermal conditions. Very interestingly, $(H_2O_3PCH_2)_2$-$NCH_2C_6H_4COOH$ showed another in situ bond cleavage behavior. Thus, a C−N bond is cleaved under reaction conditions, and with Ba^{2+} reacting with the resulting iminobis(methylphosphonic acid), $(H_2O_3PCH_2)_2NH$, a microporous open-framework compound is formed.[29]

Acknowledgment. The authors thank Dr. P. Mayer for the acquisition of the single-crystal data.

Supporting Information Available: X-ray crystallographic files in CIF format for the structure determination of $Co_2[(O_3PCH_2)_2$-$NCH_2C_6H_4COOH]\cdot H_2O$ (**1**) and $Co[(O_3PCH_2)(OCH)NCH_2C_6H_4$-$COOH]\cdot H_2O$ (**2**), reaction parameters, and photographs of $[Co_2(O_3PCH_2)_2NCH_2C_6H_4{-}COOH]\cdot 3.5H_2O$ (**4**) (before and after thermal treatment). This material is available free of charge via the Internet at http://pubs.acs.org. CCDC 274556 (compound **1**) and CCDC 274555 (compound **2**) contain the supplementary crystallographic data for this paper. These data can be obtained free of charge from The Cambridge Crystallographic Data Centre via www.ccdc.cam.ac.uk/data_request/cif.

IC0505089

(29) Bauer, S.; Müller, H.; Bein, T.; Stock, N. To be published.